

Synthetic Multienzyme Complexes Assembled on Virus-like Particles for Cascade Biosynthesis *In Cellulo*

Qixin Wei, Sicong He, Jianan Qu, and Jiang Xia*



Cite This: *Bioconjugate Chem.* 2020, 31, 2413–2420



Read Online

ACCESS |



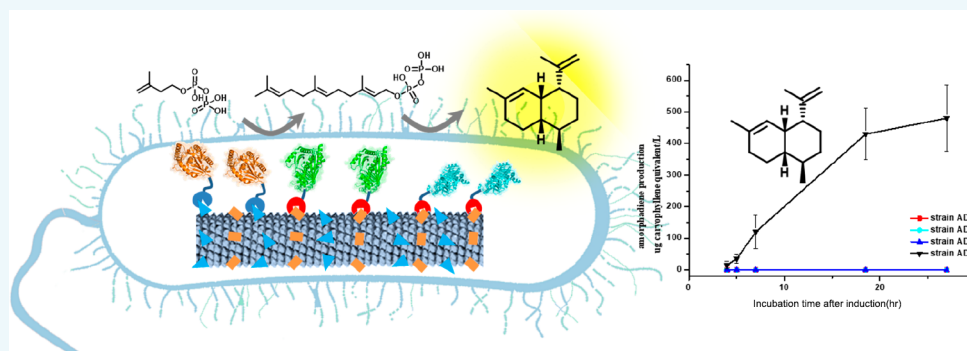
Metrics & More



Article Recommendations



Supporting Information



ABSTRACT: Multienzyme complexes, or metabolons, are natural assemblies or clusters of sequential enzymes in biosynthesis. Spatial proximity of the enzyme active sites results in a substrate channeling effect, streamlines the cascade reaction, and increases the overall efficiency of the metabolic pathway. Engineers have constructed synthetic multienzyme complexes to acquire better control of the metabolic flux and a higher titer of the target product. As most of these complexes are assembled through orthogonal interactions or bioconjugation reactions, the number of enzymes to be assembled is limited by the number of orthogonal interaction or reaction pairs. Here, we utilized the *Tobacco mosaic virus* (TMV) virus-like particle (VLP) as protein scaffold and orthogonal reactive protein pairs (SpyCatcher/SpyTag and SnoopCatcher/SnoopTag) as linker modules to assemble three terpene biosynthetic enzymes in *Escherichia coli*. The enzyme assembly switched on the production of amorphadiene, whereas the product was undetectable in all the controls without assembly. This work demonstrates a facile strategy for constructing scaffolded catalytic nanomachineries to biosynthesize valuable metabolites in bacterial cells, and a unique assembly induced the switch-on mechanism in biosynthesis for the first time.

INTRODUCTION

In nature, cells have developed multienzyme complexes of sequential enzymes to regulate signal transduction and streamline metabolic conversion. One classical example is pyruvate dehydrogenase multienzyme complex, which exhibits an elegant structure consisting of three enzymes to convert pyruvate into acetyl-coenzyme A.¹ In the multienzyme complex, active sites of the enzymes are clustered in close proximity that allows the metabolic intermediates to be directly channeled from one enzyme to another. It avoids the unwanted diffusion of intermediates into cytosol, the leakage of toxic intermediates, and the interferential competing enzymatic reactions.^{2–5} Therefore, from the aspect of cascade catalysts, the overall reaction rate can be increased by the enzyme assembly.^{6–8}

Aiming at increasing the titer of heterologous biosynthesis and attaining a greater control of the metabolic flux, synthetic multienzyme complexes have been engineered *in cellulo*. Focusing on terpene biosynthesis, we reported covalent assembly of sequential enzymes in mevalonate pathway that

led to increased production of lycopene and astaxanthin,⁹ as well as assembly of the isoprene isomerase with the first dedicated enzyme in terpene biosynthetic pathway.¹⁰ These achievements set the stage for us to extend the enzyme assembly strategies to scaffolded assembly to accommodate more enzymes, and to different terpene products, for example, amorphadiene, the key precursor to artemisinin which is a valuable and powerful drug against malaria. Artemisinin is a sesquiterpene lactone peroxide that can be extracted in natural plant, however, with limited yield. As the precursor molecules, amorphadiene can convert to artemisinin with relatively few chemical processes. Meanwhile, amorphadiene can

Received: August 24, 2020

Revised: September 20, 2020

Published: October 1, 2020



be produced in microorganism such as *E. coli* by introducing the heterologous biosynthetic pathway.¹¹

Scaffolded assembly is a convenient way for modular construction of multienzyme complexes.^{6,12–16} For example, Dueber et al. developed a modular assembly by constructing synthetic protein scaffolds to accommodate three sequential enzymes in the mevalonate biosynthesis pathway based on protein–protein interactions between SH3, SH2, and PDZ domains.¹⁷ This strategy has shown its generality to control the metabolic flux in metabolic engineering.^{18–24} Although the stoichiometry of the assembly state can be accurately controlled in this case, the capacity of the scaffold is very limited. To expand the capacity of the scaffold, we reason that *Tobacco Mosaic Virus* (TMV) virus-like particles (VLPs) would be a great candidate as it harbors thousands of the binding sites, if each VLP monomer is engineered to present one binding site. Typically, TMV VLPs consist of more than two thousand copies of the monomer, the coat protein (CP), as CPs self-assemble into a helical rod-like structure with a size of 300 nm in length and 18 nm in diameter.²⁵ Previous studies also reported that peptide tags can be genetically fused to the CP and allow the tags to be displayed on the surface of VLPs.²⁶

Genetically encoded click reactions provide a perfect tool in constructing the covalently linked protein complexes.²⁷ For example, SpyTag and SpyCatcher are two protein fragments generated by splitting an adhesin protein FbaB that contains an isopeptide bond and was originally found in bacteria.²⁸ These two fragments can spontaneously react to reconstitute the intermolecular isopeptide linkage, thereby covalently linking the two fragments together *in vitro* and *in vivo*.^{29,30} Further, another covalently reacting pair SnoopTag/SnoopCatcher was engineered and found to be orthogonal with the SpyTag/SpyCatcher pair.³¹ Inspired by the *in cellulo* reactivity of these two pairs, we recently reported the construction of covalent multienzyme complexes of the mevalonate pathway inside bacterial cells using these four fragments as tags in a scaffold-free strategy, and observed a significant increase of the production of carotenoids.⁹ Here, we engineer the CP to self-assemble to TMV VLPs with surface-displayed protein reaction sites, and use these engineered VLPs as scaffolds to assemble three enzymes in the amorpha-4,11-diene biosynthetic pathway, isopentenyl diphosphate isomerase (Idi), FPP synthase (IspA), and amorpha-4,11-diene synthase (ADS) through site-specific covalent reactions between SpyCatcher and SpyTag, and SnoopCatcher and SnoopTag (Figure 1). This scaffold-supported multienzyme complex was expressed in the bacterial cell *E. coli* for the production of amorpha-4,11-diene, the key precursor of artemisinin.

RESULTS

Engineering Coat Proteins for Assembly of VLPs in Bacterial Cells. TMV VLPs are nanorods self-assembled by a single protein, called the coat protein (CP). Two negatively charged residues E55 and D77 were substituted by neutral amino acids Q and N, respectively (sequence shown in Figure S1 in the Supporting Information), which stabilizes the quaternary structure of the helical rod shape.³² The structure of a single coat CP (Figure 2A) has been elucidated, providing a blue print to genetically install interaction sites, without compromising its expression or self-assembly in bacterial cells. The crystal structure of CP shows that both N and C termini are close to each other, and extend outside of the assembly core, which infers that genetic modification at either terminus

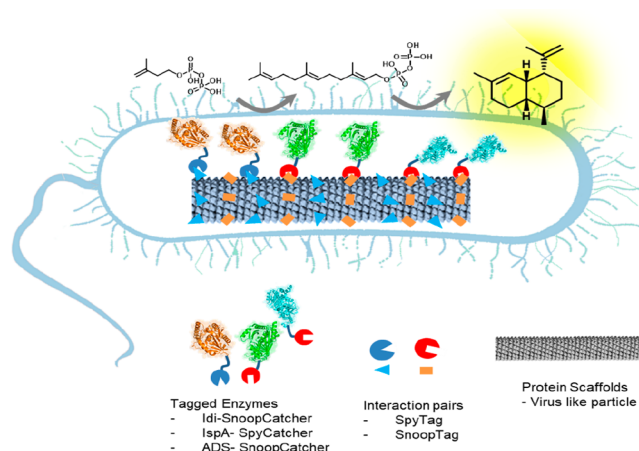


Figure 1. Schematic illustration showing the design and construction of multienzyme complexes inside bacterial cells to facilitate cascade biosynthesis from IPP to FPP to amorpha-diene.

will not interfere the assembly, or the property of the tag. We first used a His-tag (6× histidine) as a model to test whether C-terminal tag affects the self-assembly of CP. CP-His (6× histidine added at the C-terminus of the single coat protein) was cloned and overexpressed in *E. coli*. The formation of virus-like particle was visualized by transmission electron microscopy (TEM) (Figure 2B and C). A rod-shaped structure with lengths of hundreds of nanometers indicated that C-terminal tagging of the self-assembly of CP to form VLPs. The scaffold therefore can be constructed.

VLP-Scaffolded Assembly of Fluorescent Proteins, a Model System. We next assembled fluorescent proteins cyan fluorescent protein (CFP) and yellow fluorescent protein (YFP) on VLPs. In our design, Spytag-SnoopCatcher and SnoopTag-SnoopCatcher described previously serve as the linker module between enzyme and protein scaffold in the system. Those four reactive moieties were fused to the C-terminus of VLP, CFP, and YFP, respectively, to give CP-SpyTag, CP-SnoopTag, CFP-SpyCatcher, and YFP-SnoopCatcher. The four proteins were coexpressed inside *E. coli* to allow scaffolded assembly: CP-SpyTag will specifically react with CFP-SpyCatcher, CP-SnoopTag will specifically react with YFP-SnoopCatcher, and CP-SpyTag will self-assemble with CP-SnoopTag (Figure 3A and Figure S2). The fluorescence energy transfer between CFP and YFP was measured under fluorescence lifetime imaging (FLIM). The CFP lifetime of the cells that express the enzyme complex (Figure 3B, column 3) was significantly lower than the one expressing the individual enzymes without the VLP scaffold, or with VLPs but no interacting motifs (Figure 3B, column 1 and column 2, respectively). The distance between CFP and YFP was 6.5 nm estimated from the FRET efficiency. This indicates that CFP and YFP in the protein complex are assembled into close proximity *in cellulo*. Altogether, this experiment validated that CFP and YFP proteins have been coassembled into VLP scaffolds through site-specific protein reactions.

Synthetic Multienzyme Complexes for Amorpha-4,11-diene Biosynthesis. After validating the complex formation in the model system, we next turned to the cascade biosynthesis of amorpha-4,11-diene, an important terpene product and precursor of the drug artemisinin. Two pathways are required together to produce amorpha-4,11-diene. The

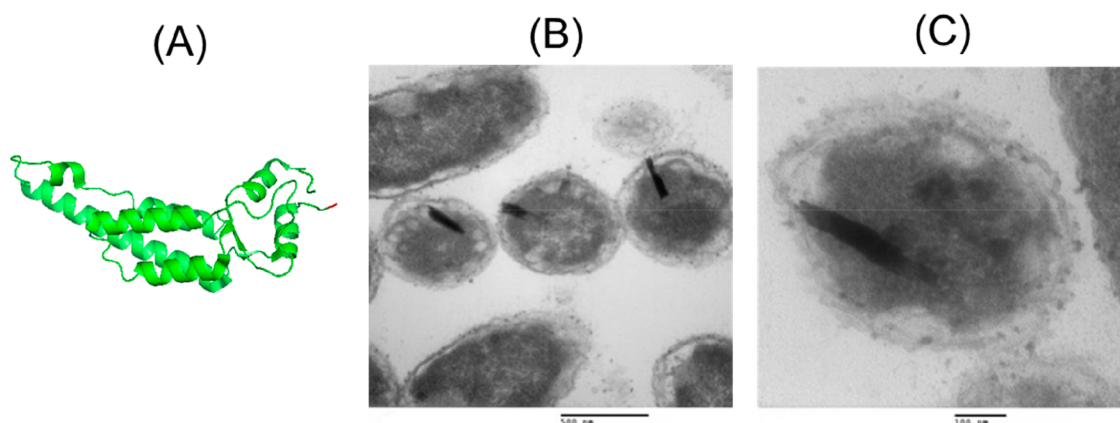


Figure 2. Engineering CP protein at the C-terminus does not affect the formation of VLP in *E. coli* cells. (A) Crystal structure of the *Tobacco Mosaic Virus* coat protein (PDB: 6ISA). The C-terminus is labeled in red. (B,C) Different magnifications of TEM images of VLP nanorods formed by CP-His in *E. coli*. (B) Scale bar, 500 nm. (C) Scale bar, 100 nm.

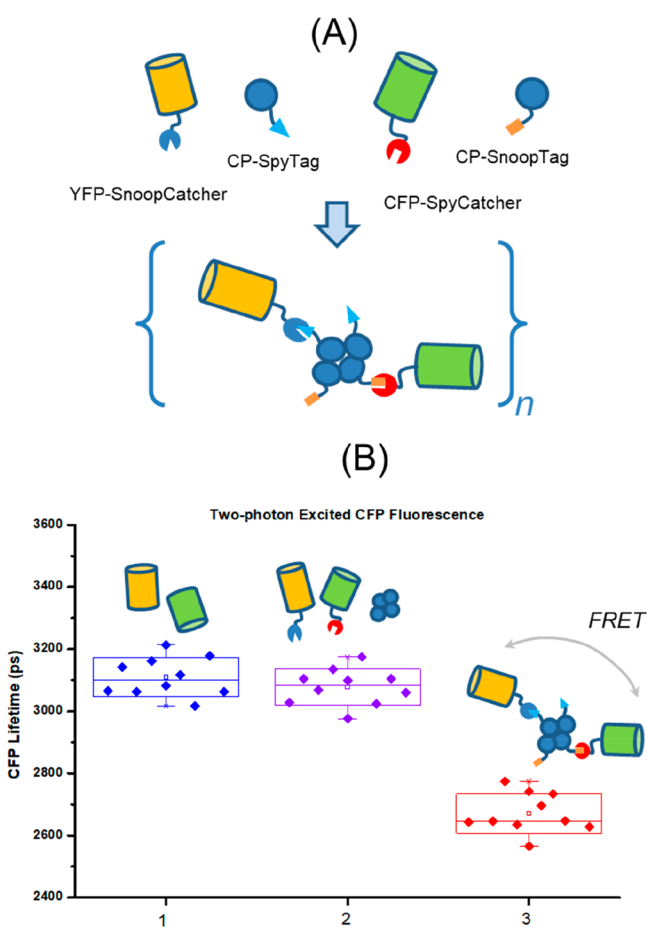


Figure 3. Scaffolded assembly of the fluorescent proteins on virus-like particles in *E. coli* cells. (A) Schematic illustration showing the design and construction of CFP and YFP on VLP. (B) Measurement of CFP lifetime of the three bacterial strains by fluorescence lifetime microscope. Column 1, the strain expressing untagged CFP and YFP only. Column 2, the strain expressing tagged CFP and YFP and the untagged CP, which does not form assemblies. Column 3, the strain expressing the multienzyme complex. The FRET effect indicated by the decreased CFP lifetime indicates successful assembly.

methyl D-erythritol 4-phosphate (MEP) pathway exists originally in bacterial cells to provide the five carbon building units, isopentenyl pyrophosphate (IPP), and its allylic isomer

dimethylallyl pyrophosphate (DMAPP), which serve as the basis for the biosynthesis of terpenoids. The second pathway involves three enzymes that convert IPP and DMAPP to terpenoids: isopentenyl diphosphate isomerase (Idi), farnesyl pyrophosphate synthase (IspA), and amorpha-4,11-diene synthase (ADS). Idi is an isomerase that catalyzes the reversible conversion of IPP and DMAPP, which is the critical reaction that links the MEP pathway with the downstream amorpha-4,11-diene biosynthetic pathway. IspA is responsible for the condensation of IPP and DMAPP to produce farnesyl diphosphate (FPP), which is then further isomerized by amorpha-4,11-diene synthase to generate the final product amorpha-4,11-diene.

We transformed a heterologous pathway including Idi, IspA, and ADS into *E. coli* to realize amorpha-4,11-diene biosynthesis: the downstream terpene biosynthetic pathway in cytosol responsible for condensing IPP and DMAPP sequentially to amorpha-4,11-diene (Figure 4). The MEP pathway links with the downstream pathway by a critical reaction, the reversible interconversion between IPP and DMAPP catalyzed by Idi. The supply of these two starting materials poses a bottleneck to the downstream biosynthesis and excess supply can enhance the production yield.³³ However, high levels of IPP and DMAPP are known as cytotoxicity compounds^{34,35} that might inhibit cell growth and also the production titers. We envision that assembling Idi, IspA, and ADS together will streamline these three enzymes and promote the production of amorpha-4,11-diene. It has been proven that Idi plays an important role in terpene synthesis, such as lycopene,³⁶ taxadiene,³⁷ farnesene,³⁸ etc. For example, fusion of IspA and α -farnesene synthase can increase the farnesene production yield.³⁹ Moreover, it is suggested that ADS is also a rate-limiting enzyme.⁴⁰ We reason that assembly of Idi, IspA, and ADS will directly channel IPP/DMAPP to the desired final product amorpha-4,11-diene.

Similar to the previous model system, all binding pairs were fused at the C-terminus of enzymes: CP-SpyTag, CP-SnoopTag, Idi-SnoopCatcher, IspA-SpyCatcher, and ADS-SnoopCatcher. These three catalytic enzymes will react covalently with the coexpressed CP-SpyTag and CP-SnoopTag, which then self-assembled as the multienzyme complex in a rod-shaped structure. Those enzymes were cloned into one plasmid, which was then transformed into *E. coli* to give bacterial strains AD 0 to AD 3 (Figure 5A). AD 0 is

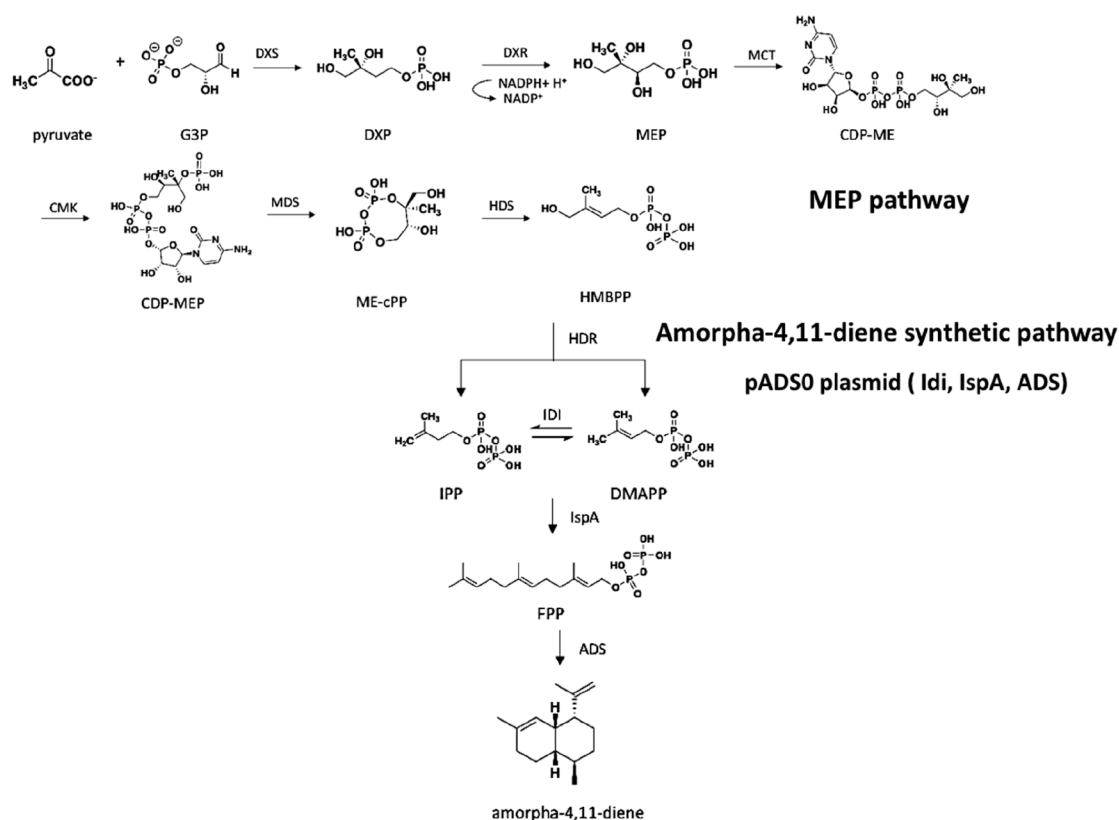


Figure 4. Schematic illustration of the amorphadiene biosynthesis pathways, including the plasmid used in this study. MEP pathway is an endogenous pathway in *E. coli*.

a base strain in which only expressing the unmodified enzymes Idi, IspA, and ADS. AD 1 contains additional unmodified protein scaffold CP. AD 2 expresses both the modified enzymes (Idi-SnoopCatcher, IspA-SpyCatcher, and ADS-SnoopCatcher), as well as the unmodified CP, in which all the enzymes are still in free-floating form. AD 3 is the strain that forms the multienzyme complex by coexpressing Idi-SnoopCatcher, IspA-SpyCatcher, ADS-SnoopCatcher, CP-SpyTag, and CP-SnoopTag. Since CP and CP-SpyTag were fused with N-terminal Histag, Western blot analysis was also done to verify the successful formation of IspA-SpyCatcher with CP-SpyTag (Figure S3). Although the yield of the covalent reactions inside the cell could not be quantitatively measured, this data shows that the covalent reaction did take place *in cellulo*.

We next evaluated the amorphadiene production titer of four strains. The same condition was used for all these strains and IPTG was added at the same OD value. The growth of all the strains was similar (Figure 5B), indicating that multienzyme complex formation did not pose any harm to the growth of the bacterial cells. The cell cultures were extracted, and the organic layer was examined for the presence and the quantity of amorphadiene by GC/MS. Only strain AD 3, the assembly strain, showed the production of amorphadiene (Figure 5C). No amorphadiene was found in other three unassembled strains, AD 0, AD 1, and AD 2. The extraction product was confirmed to be amorphadiene by gas chromatogram–mass spectrometry (GC-MS). The enzymatic product elutes at 4.37 min (Figure 6A). The mass spectrum of this peak corresponds well with the reported spectrum of amorphadiene (Figure 6B).⁴¹ Consistent with the previous studies, the most abundant peak is the one

with m/z of 119, followed by the second and third abundant peak at m/z of 93.05 and m/z of 189.1, respectively. Three ionized fragments were also found in the fingerprint, *Fragment a* formed by cleavage of methyl group; *Fragment b* formed by cleavage of both the C-6/C-7 and C-9/C-10 bonds, and *Fragment c* formed by cleavage of the C-6/C-7 and C-1/C-10 bonds.⁴² These results confirmed that the enzymatic product from the modified strain AD 3 is the desired compound, amorphadiene. Altogether, a comparison of four strains show that scaffolded assembly of Idi, IspA, and ADS is the *sine qua non* of the successful production of amorphadiene, or, in other words, assembly of these three downstream terpene biosynthetic enzymes “switches on” the biosynthesis of amorphadiene in bacterial cells.

CONCLUSIONS

Scaffolded assembly of sequential metabolic enzymes is known to be an effective way to control the metabolic flux and the biosynthesis titer. A scaffold that is generally applicable and has high capacity to accommodate multiple enzymes is favorable. Here, we demonstrated the scaffolded assembly of a multienzyme complex that switches on the biosynthesis of amorphadiene in *E. coli*. Virus-like particles assembled by the coat protein (CP) derived from TMV were engineered as the protein scaffold inside cells, and site-specific protein reactive pairs were chosen as the linker modules. Genetic engineering of the CP monomer allows the reactive sites to be displayed on the surface of VLPs. Enzymes in terpene biosynthetic pathway, Idi, IspA, and ADS were engineered with the reactive tags to form the complex on the VLP protein scaffold. Only the strain

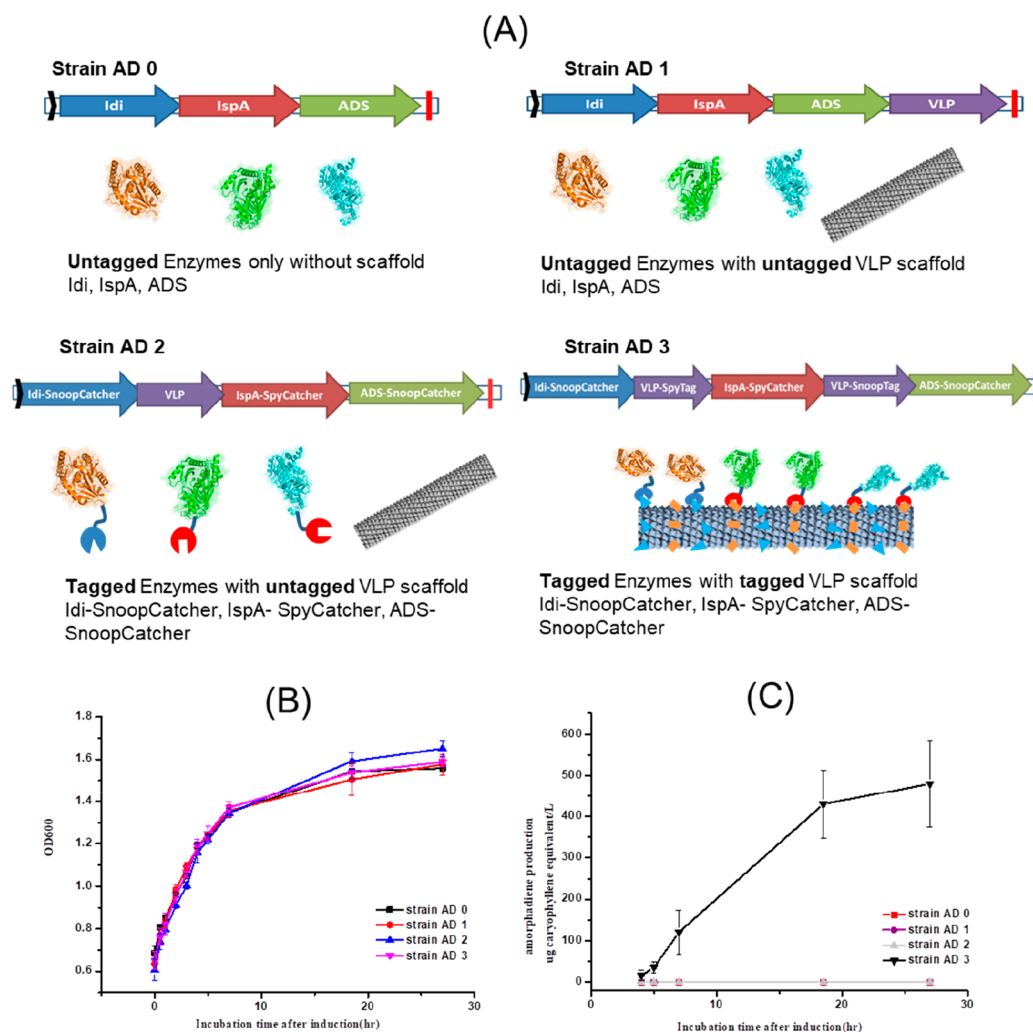


Figure 5. Synthetic multienzyme complexes switch on the production of amorpha-4,11-diene biosynthesis in *E. coli*. (A) Schematic illustration showing the construction of the production strains. (B) Comparison of the growth profile of strains AD 0 to AD 3. (C) Comparison of the amorpha-4,11-diene titers of strains AD 0 to AD 3. Concentration of amorpha-4,11-diene was quantified using caryophyllene as a reference and caryophyllene equivalent as the concentration unit.

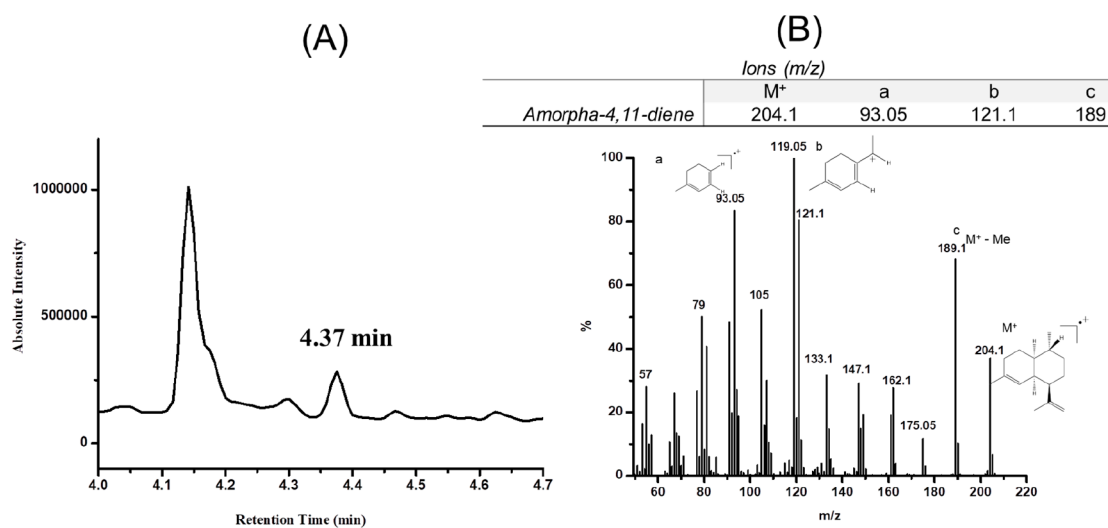


Figure 6. GC-MS analysis of the product from the strain AD 3 supports the successful production of amorpha-4,11-diene. (A) Gas chromatogram showing the peak at 4.37 min only in the strain AD 3. (B) Mass spectrum of the peak at 4.37 min shows the correct mass spectrometric signals of the parent and fragment ions.

expressing the multienzyme complex showed the production of desired product, amorpha-4,11-diene.

This work, first of all, showcases a general strategy for successful formation of the synthetic multienzyme complex *in cellulo*. Second, this enzyme complex switches on the biosynthesis of amorpha-4,11-diene, the first example of “assembly-induced production” to the best of our knowledge. Surprisingly, strains AD 0, AD 1, and AD 2 did not produce any detectable level of amorpha-4,11-diene. We reason that possibly the endogenous MEP pathway produces a low level of IPP and DMAPP in *E. coli* only sufficient to sustain the normal physiology of the cells. The terpene biosynthetic pathway that we introduced through heterologous source does not have sufficient amount of IPP and DMAPP in strains AD 0, AD 1, and AD 2 to produce the terpene product. Neither could this pathway compete with the endogenous consumers of the C5 precursors. Strain AD 3, however, shows a robust production of the terpene product, possibly because the assembly of the three enzymes (Idi, IspA, and ADS) streamlines the reaction of IPP and DMAPP toward terpene biosynthesis, significantly increases the overall efficiency of this pathway, and thus leads to the production of amorpha-4,11-diene. The exact mechanism of how multienzyme assembly promotes cascade biosynthesis, however, is under debate. For example, Hess and co-workers presented evidence that the proximity does not contribute to activity enhancement in certain multienzyme cascades.^{43,44} Unlike the cascade reactions carried out in the test tube using purified model enzymes with well-understood kinetics, the delineation of the multienzyme kinetics in our system is difficult because of the complexity of the *in cellulo* environment and the intertwined metabolic network of the cell. Nevertheless, our serendipitous discovery that multienzyme assembly on TMV VLP can significantly promote the production of amorpha-4,11-diene in *E. coli* presents one example of assembly induced catalytic “turn-on” effect.

MATERIALS AND METHODS

Materials and Instruments. CP-His gene and PCR primers were synthesized by Beijing Genomics Institute (Shenzhen, China). SpyCatcher and SpyTag genes were kind gifts from Prof. Sun Fei of Hong Kong University of Science and Technology. SnoopCatcher and SnoopTag genes were synthesized by Beijing Genomics Institute (Shenzhen, China). DNA sequencing was also obtained by Beijing Genomics Institute (Shenzhen, China). LB broth and agarose were purchased from USB. Glycerol was purchased from Invitrogen by Thermo Fisher Scientific. Dodecane was purchased from J&K Chemical. Sodium chloride was purchased from Scharlau Chemicals. Yeast extract and tryptone were purchased from OXOID Company. Takara EmeraldAmp GT PCR Master Mix was used for PCR and Thermo FastDigest enzymes was used for restriction enzyme digest. DNA fragments were purified by gel electrophoresis using Bio-Rad DNA Electrophoresis Cells & Systems and extracted through Monarch DNA Gel Extraction Kit from New England Biolabs (UK) Ltd. Ligation was carried out by a Thermo T4 DNA ligase and the corresponding buffer. Homemade competent cell XL.Blue or Top 10 and BL21 (DE3) were used to transform the plasmids for plasmid construction and protein expression. Culture plates were purchased from SPL Life Sciences. Optical density was detected on UV-1100 Spectrophotometer from NAPADA Instruments. Amorpha-4,11-diene was detected on a GCMS-Q2010 Plus (Shimadzu Corporation, Japan).

Plasmid Construction for Multienzyme Complex with Model Enzyme. CP-SpyTag was prepared through the digestion and ligation process. Briefly, VLP was amplified with designed primers that introduced restriction enzyme recognition sites *Bam*HI and *Hind*III, respectively. The gene of SpyTag encoding a N-terminal (GGGS)₂ linker sequence was synthesized by Beijing Genomics Institute (*S'* *Hind*III and *3'* *Not*I were incorporated into the sequence). The double enzyme digested genes were inserted into the MCS-1 part of pACYC-Duet and the similarly prepared gene CP-SnoopTag was then inserted into the MCS-2 to get the final construct pACYC-CP-SpyTag-CP-SnoopTag. Another plasmid pET-YFP-SpyCatcher-CFP-SnoopCatcher was constructed similarly.

Lifetime-Based Fluorescence Resonance Energy Transfer (FRET). FRET can be served as a molecular ruler based on its sensitivity in the range of 2–10 nm. It is a nonradiative process that the energy transferred from an excited fluorescent molecule (donor) to a nonexcited fluorophore (acceptor). The energy transfer results in the decreasing fluorescence lifetime of the donor. FRET efficiency can be obtained by comparing the donor lifetimes in the absence and presence of the acceptor. The FRET efficiency E as a measure of the donor quenching can be calculated as $E = 1 - (\tau_{DA}/\tau_D)$ (τ_{DA} = Lifetime of the donor in the presence of the acceptor, τ_D = Lifetime of the donor without acceptor). The fluorescence lifetime of CFP (donor) was measured by a home-built two-photon fluorescence lifetime imaging microscope. The CFP fluorescence was excited by 810 nm femtosecond laser, and its lifetime was recorded by a time-correlated single photon counting module. The distance between CFP and YFP can be calculated by the following equation: $R = R_0 \sqrt{(1 - E)/E}$ (R_0 is 5 nm for CFP/YFP pairs).

Plasmid Construction for Amorphadiene Production. Idi-SnoopCatcher gene was constructed through the simple digestion and ligation process. Briefly, the Idi was amplified, and then purified using the Monarch PCR & DNA cleanup kit to obtain the high-quality fragment. After that, the fragment was inserted into pMD19T (simple). This plasmid served as vector and the amplified fragment SnoopCatcher was digested with restriction enzyme *Hind*III and *Xho*I and ligated into the vector to get the final construct pMD19T (simple)-Idi-SnoopCatcher. The ligation solution was transformed into XL1-BLUE competent cells. A single colony was taken and the correct construct was screened out by DNA sequencing. Other genes were similarly obtained, and finally these fragments were prepared: Idi-SnoopCatcher, CP-SpyTag, IspA-SpyCatcher, CP-SnoopTag, and ADS-SnoopCatcher. GENEWIZ Limited helped to assemble those fragments into the vector part of plasmid pFZ 71 to build the final construct pADS1.

Plasmid pADS0 encoding the genes of non-engineered enzymes was built through Gibson Assembly Strategy. Briefly, fragment 1 with the genes Idi, fragment 2 with the genes IspA, fragment 3 with the genes ADS, and fragment 4 containing the vector part of plasmid pFZ 71 were all obtained from PCR using designed primers. Overlap regions were designed between fragment 1 and fragment 2, fragment 2 and fragment 3, fragment 3 and fragment 4, as well as fragment 4 and fragment 1. Gibson assembly was then used to ligate those fragments together and get the final construct, plasmid pADS0. Plasmid pADSC1 was done by inserting the fragment CP into pADS0 with restriction enzyme *Sac*I and *Xho*I.

Amorphadiene Production and Quantification. The amorphadiene production strain AD 0, strain AD 1, strain AD 2, and strain AD 3 were constructed by electroporation of plasmid pADS0, pADSC 1, pADSC 2, and pADS1 into *E. coli* BL21(DE3) competent cell. The starting cultures were prepared by picking up single colony of each strains into 3 mL of LB supplemented with 100 µg/mL ampicillin and grown overnight in 37 °C. After that, 1.5 mL of start culture was inoculated into a conical flask containing 150 mL of 2 × YT medium (16 g tryptone, 10 g yeast extract, 5 g sodium chloride per liter, pH adjusted to 7.0 by 5 N NaOH) at 37 °C with 100 µg/mL ampicillin and 2% glycerol. IPTG was added to the final concentration of 0.1 mM until the optical density 600 nm (OD₆₀₀) reached 0.6–0.8, and the culture temperature decreased to 30 °C. The medium was overlaid with 5 mL dodecane 3 h later, and cells continued to grow at the same condition to produce amorphadiene. 400 µL of emulsifier sample was taken at designated intervals. After being centrifuged at 13,000 g for 3 min, the supernatant was collected and subjected to gas chromatography–mass spectrometry (GC-MS) for further analysis.

The production of amorphadiene was quantified in total ion scan mode on a RTX-5 MS column (inner diameter, 0.25 mm; length, 30.0 m; film thickness, 0.25 µm). Samples of 1 µL were injected in a split ratio of 1:3. The injector temperature was 250 °C, and the oven temperature was initially held at 160 °C for 2 min, following by increasing at a rate of 15 °C/min to 250 °C and held for another 2 min. Helium served as the carrier gas at the flow of 6.6 mL/min with an inlet pressure of 86.7 kPa. Amorphadiene concentrations were converted to caryophyllene equivalents using a caryophyllene standard curve.

■ ASSOCIATED CONTENT

Supporting Information

The Supporting Information is available free of charge at <https://pubs.acs.org/doi/10.1021/acs.bioconjchem.0c00476>.

Detailed experimental procedures; Plasmids used in this study; Strain used in this study; DNA sequence information on all the enzymes and proteins used in this study; Protein sequence of CP-His; Confocal image of strains expressing tagged CFP and YFP with or without VLP scaffold in *E. coli*; Western blots for strains AD2 and AD3; Standard curve of caryophyllene (PDF)

■ AUTHOR INFORMATION

Corresponding Author

Jiang Xia – Department of Chemistry, The Chinese University of Hong Kong, Shatin, Hong Kong SAR, China; orcid.org/0000-0001-8112-7625; Phone: (852) 3943 6165; Email: jiangxia@cuhk.edu.hk; Fax: (852) 2603 5057

Authors

Qixin Wei – Department of Chemistry, The Chinese University of Hong Kong, Shatin, Hong Kong SAR, China

Sicong He – Department of Electronic and Computer Engineering, Center of Systems Biology and Human Health, School of Science and Institute for Advanced Study, Hong Kong University of Science and Technology, Kowloon, Hong Kong SAR, China

Jianan Qu – Department of Electronic and Computer Engineering, Center of Systems Biology and Human Health,

School of Science and Institute for Advanced Study, Hong Kong University of Science and Technology, Kowloon, Hong Kong SAR, China; orcid.org/0000-0002-6809-0087

Complete contact information is available at:

<https://pubs.acs.org/10.1021/acs.bioconjchem.0c00476>

Author Contributions

Q. W. and J. X. conceived of the project, designed experiments, and wrote the manuscript. Q. W. and S. H. carried out the experiments. J. Q. helped analyze the data.

Notes

The authors declare no competing financial interest.

■ ACKNOWLEDGMENTS

This work was partially funded by grants by University Grants Committee of Hong Kong (GRF grants 14304915, 14321116, 14306317, 14307218).

■ REFERENCES

- (1) Patel, M. S., Nemeria, N. S., Furey, W., and Jordan, F. (2014) The pyruvate dehydrogenase complexes: structure-based function and regulation. *J. Biol. Chem.* 289, 16615–16623.
- (2) Huang, X., Holden, H. M., and Raushel, F. M. (2001) Channeling of Substrates and Intermediates in Enzyme-Catalyzed Reactions. *Annu. Rev. Biochem.* 70, 149–180.
- (3) Miles, E. W., Rhee, S., and Davies, D. R. (1999) The Molecular Basis of Substrate Channeling. *J. Biol. Chem.* 274, 12193–12196.
- (4) Wheeldon, I., Minter, S. D., Banta, S., Barton, S. C., Atanassov, P., and Sigman, M. (2016) Substrate Channeling as an Approach to Cascade Reactions. *Nat. Chem.* 8, 299–309.
- (5) Zhang, Y.-H. P. (2011) Substrate Channeling and Enzyme Complexes for Biotechnological Applications. *Biotechnol. Adv.* 29, 715–725.
- (6) Conrado, R. J., Varner, J. D., and DeLisa, M. P. (2008) Engineering the Spatial Organization of Metabolic Enzymes: Mimicking Nature's Synergy. *Curr. Opin. Biotechnol.* 19, 492–499.
- (7) Siu, K.-H., Chen, R. P., Sun, Q., Chen, L., Tsai, S.-L., and Chen, W. (2015) Synthetic Scaffolds for Pathway Enhancement. *Curr. Opin. Biotechnol.* 36, 98–106.
- (8) Whitaker, W. R., and Dueber, J. E. (2011) Metabolic Pathway Flux Enhancement by Synthetic Protein Scaffolding. *Methods Enzymol.* 497, 447–468.
- (9) Qu, J., Cao, S., Wei, Q., Zhang, H., Wang, R., Kang, W., Ma, T., Zhang, L., Liu, T., Au, S. W. N., et al. (2019) Synthetic multienzyme complexes, catalytic nanomachineries for cascade biosynthesis in vivo. *ACS Nano* 13 (9), 9895–9906.
- (10) Kang, W., Ma, T., Liu, M., Qu, J., Liu, Z., Zhang, H., Shi, B., Fu, S., Ma, J., Lai, L. T. F., et al. (2019) Modular enzyme assembly for enhanced cascade biocatalysis and metabolic flux. *Nat. Commun.* 10, 4247.
- (11) Martin, V. J. J., Pitera, D. J., Withers, S. T., Newman, J. D., and Keasling, J. D. (2003) Engineering a mevalonate pathway in *Escherichia coli* for production of terpenoids. *Nat. Biotechnol.* 21 (7), 796–802.
- (12) Küchler, A., Yoshimoto, M., Luginbühl, S., Mavelli, S., and Walde, P. (2016) Enzymatic reactions in confined environments. *Nat. Nanotechnol.* 11, 409–420.
- (13) Kerfeld, C. A. (2017) A bioarchitectonic approach to the modular engineering of metabolism. *Philos. Trans. R. Soc., B* 372, 20160387.
- (14) Pröschel, M., Detsch, R., Boccacini, A. R., and Sonnewald, U. (2015) Engineering of metabolic pathways by artificial enzyme channels. *Front. Bioeng. Biotechnol.* 3, 168.
- (15) Horn, A. H. C., and Sticht, H. (2015) Synthetic protein scaffolds based on peptide motifs and cognate adaptor domains for improving metabolic productivity. *Front. Bioeng. Biotechnol.* 3, 191.

- (16) Lee, H., DeLoache, W. C., and Dueber, J. E. (2012) Spatial organization of enzymes for metabolic engineering. *Metab. Eng.* 14, 242–251.
- (17) Dueber, J. E., Wu, G. C., Malmirchegini, G. R., Moon, T. S., Petzold, C. J., Ullal, A. V., Prather, K. J., and Keasling, J. D. (2009) Synthetic Protein Scaffolds Provide Modular Control over Metabolic Flux. *Nat. Biotechnol.* 27, 753–9.
- (18) Moon, T. S., Dueber, J. E., Shiue, E., and Prather, K. L. (2010) Use of modular, synthetic scaffolds for improved production of glucaric acid in engineered *E. Coli*. *Metab. Eng.* 12, 298–305.
- (19) Moon, T. S., Yoon, S. H., Lanza, A. M., Roy-Mayhew, J. D., and Prather, K. L. (2009) Production of glucaric acid from a synthetic pathway in recombinant *Escherichia coli*. *Appl. Environ. Microbiol.* 75, 589–595.
- (20) Agapakis, C. M., Ducat, D. C., Boyle, P. M., Wintermute, E. H., Way, J. C., and Silver, P. A. (2010) Insulation of a synthetic hydrogen metabolism circuit in bacteria. *J. Biol. Eng.* 4, 3.
- (21) Baek, J. M., Mazumdar, S., Lee, S. W., Jung, M. Y., Lim, J. H., Seo, S. W., Jung, G. Y., and Oh, M. K. (2013) Butyrate production in engineered *Escherichia coli* with synthetic scaffolds. *Biotechnol. Bioeng.* 110, 2790–2794.
- (22) Wang, Y., and Yu, O. (2012) Synthetic scaffolds increased resveratrol biosynthesis in engineered yeast cells. *J. Biotechnol.* 157, 258–260.
- (23) Zhao, S., Jones, J. A., Lachance, D. M., Bhan, N., Khalidi, O., Venkataraman, S., Wang, Z., and Koffas, M. A. G. (2015) Improvement of catechin production in *Escherichia coli* through combinatorial metabolic engineering. *Metab. Eng.* 28, 43–53.
- (24) Li, J., Nayak, S., and Mrksich, M. (2010) Rate enhancement of an interfacial biochemical reaction through localization of substrate and enzyme by an adaptor domain. *J. Phys. Chem. B* 114, 15113–15118.
- (25) Koch, C., Eber, F. J., Azucena, C., Forste, A., Walheim, S., Schimmel, T., Bittner, A. M., Jeske, H., Gliemann, H., Eiben, S., Geiger, F. C., Wege, C., et al. (2016) Novel roles for well-known players: from tobacco mosaic virus pests to enzymatically active assemblies. *Beilstein J. Nanotechnol.* 7, 613–629.
- (26) Zang, F., Gerasopoulos, K., Brown, A. D., Culver, J. N., and Ghodssi, R. (2017) Capillary microfluidics-assembled virus-like particle bionanoreceptor interfaces for label-free biosensing. *ACS Appl. Mater. Interfaces* 9 (10), 8471–8479.
- (27) Sun, F., and Zhang, W. B. (2017) Unleashing chemical power from protein sequence space toward genetically encoded “click” chemistry. *Chin. Chem. Lett.* 28 (011), 2078–2084.
- (28) Zakeri, B., Fierer, J. O., Celik, E., Chittock, E. C., Schwarz-Linek, U., Moy, V. T., and Howarth, M. (2012) Peptide tag forming a rapid covalent bond to a protein, through engineering a bacterial adhesin. *Proc. Natl. Acad. Sci. U. S. A.* 109 (12), E690–7.
- (29) Reddington, S. C., and Howarth, M. (2015) Secrets of a covalent interaction for biomaterials and biotechnology: SpyTag and SpyCatcher. *Curr. Opin. Chem. Biol.* 29, 94–99.
- (30) Li, L., Fierer, J. O., Rapoport, T. A., and Howarth, M. (2014) Structural analysis and optimization of the covalent association between spycatcher and a peptide tag. *J. Mol. Biol.* 426 (2), 309–317.
- (31) Veggiani, G., Nakamura, T., Brenner, M. D., Gayet, R. V., and Howarth, M. (2016) Programmable polyproteins built using twin peptide superglues. *Proc. Natl. Acad. Sci. U. S. A.* 113 (5), 1202–1207.
- (32) Fan, X. Z., Naves, L., Siwak, N. P., Brown, A., Culver, J., and Ghodssi, R. (2015) Integration of genetically modified, virus-like-particles, with an optical resonator for selective bio-detection. *Nanotechnology* 26 (20), 205501.
- (33) Yoon, S.-H., Lee, S.-H., Das, A., Ryu, H.-K., Jang, H.-J., Kim, J.-Y., Oh, D.-K., Keasling, J. D., and Kim, S.-W. (2009) Combinatorial expression of bacterial whole mevalonate pathway for the production of beta-carotene in *E. coli*. *J. Biotechnol.* 140, 218–226.
- (34) George, K. W., Chen, A., Jain, A., Batth, T. S., Baidoo, E. E. K., Wang, G., Adams, P. D., Petzold, C. J., Keasling, J. D., and Lee, T. S. (2014) Correlation analysis of targeted proteins and metabolites to assess and engineer microbial isopentenol production. *Biotechnol. Bioeng.* 111, 1648–1658.
- (35) George, K. W., Thompson, M. G., Kim, J., Baidoo, E. E. K., Wang, G., Benites, V. T., Petzold, C. J., Chan, L. J. G., Yilmaz, S., Turhanen, P., et al. (2018) Integrated analysis of isopentenyl pyrophosphate (IPP) toxicity in isoprenoid-producing *Escherichia coli*. *Metab. Eng.* 47, 60–72.
- (36) Zhu, F., Lu, L., Fu, S., Zhong, X., Hu, M., Deng, Z., and Liu, T. (2015) Targeted engineering and scale up of lycopene overproduction in *Escherichia coli*. *Process Biochem.* 50, 341–346.
- (37) Bian, G., Yuan, Y., Tao, H., Shi, X., Zhong, X., Han, Y., Fu, S., Fang, C., Deng, Z., and Liu, T. (2017) Production of taxadiene by engineering of mevalonate pathway in *Escherichia coli* and endophytic fungus *Alternaria alternata* TPF6. *Biotechnol. J.* 12, 1600697.
- (38) Zhu, F., Zhong, X., Hu, M., Lu, L., Deng, Z., and Liu, T. (2014) In vitro reconstitution of mevalonate pathway and targeted engineering of farnesene overproduction in *Escherichia coli*. *Biotechnol. Bioeng.* 111, 1396–1405.
- (39) Wang, C., Yoon, S. H., Jang, H. J., Chung, Y. R., Kim, J. Y., Choi, E. S., and Kim, S. W. (2011) Metabolic engineering of *Escherichia coli* for α -farnesene production. *Metab. Eng.* 13 (6), 648–655.
- (40) Anthony, J. R., Anthony, L. C., Nowroozi, F., Kwon, G., and Keasling, J. D. (2009) Optimization of the mevalonate-based isoprenoid biosynthetic pathway in *Escherichia coli* for production of the anti-malarial drug precursor amorpha-4,11-diene. *Metab. Eng.* 11 (1), 13–19.
- (41) Chang, Y. J., Song, S. H., Park, S. H., and Kim, S. U. (2000) Amorpha-4,11-diene synthase of *Artemisia annua*: cDNA isolation and bacterial expression of a terpene synthase involved in artemisinin biosynthesis. *Arch. Biochem. Biophys.* 383 (2), 178–184.
- (42) Picaud, S., Mercke, P., He, X., Sterner, O., Brodelius, M., Cane, D. E., and Brodelius, P. E. (2006) Amorpha-4,11-diene synthase: mechanism and stereochemistry of the enzymatic cyclization of farnesyl diphosphate. *Arch. Biochem. Biophys.* 448 (1–2), 150–155.
- (43) Zhang, Y., Tsitkov, S., and Hess, H. (2016) Proximity does not contribute to activity enhancement in the glucose oxidase–horseradish peroxidase cascade. *Nat. Commun.* 7, 13982.
- (44) Zhang, Y., and Hess, H. (2017) Toward rational design of high-efficiency enzyme cascades. *ACS Catal.* 7 (9), 6018–6027.